EXPERIMENTAL AND NUMERICAL APPROACH ON FRACTURE BEHAVIOUR OF FOUR INCHES DIAMETER CARBON-MANGANESE CRACKED WELDED PIPES IN FOUR POINT BENDING

P. SÉMÉTÉ, ***Electricité De France (EDF)***

EDF Research and Development, Mechanics and Component Technology Department
Les Renardières Research Center, 77818 MORET S/ LOING, FRANCE
E-mail : Patrick.Semete@edf.fr

C. FAIDY, ***Electricité De France (EDF)***

Engineering and Construction Division, Design Department for Thermal and Nuclear Project
12-14 avenue Dutrievoz, 69628 VILLEURBANNE Cedex, France
E-mail : Claude.Faidy@edf.fr

J.L. LAUTIER, ***Electricité De France (EDF)***

Engineering and Construction Division, Design Department for Thermal and Nuclear Project
12-14 avenue Dutrievoz, 69628 VILLEURBANNE Cedex, France
E-mail : Jean-Luc.Lautier@edf.fr

Key Words: Fracture mechanics – C-Mn weld joint – Piping

EDF has conducted a research programme to demonstrate the fracture resistance of carbon-manganese welded pipes. The main task of this programme consisted of testing three four inches diameter (114.3 mm O.D.) thin welded pipes (8.56 mm thick) which are representative of those of the sites. The three pipes were loaded under four point bending at a quasi-static rate at -20°C till their maximum bending moment was reached.
This paper presents the experimental results, finite element calculations and their comparison with the simplified fracture assessment method of the RSE-M Code.

INTRODUCTION

Pipes of the auxiliary feedwater supply line of French N4 PWR are made of carbon-manganese steel. The resistance against the fast fracture of these pipes must be proved

according to the design rules. Particularly, this paper focuses on the fracture resistance of the welded joints of this line.

Indeed, the lowest operating temperature of this line is equal to 7°C. Moreover, the material can be subject to thermal ageing because of the level of in-service temperature (more than 250°C for some parts of the line). On another hand, the welded joint of those pipes are not stress-relieved according to the industrial practice for small wall thickness.

So, the proof has to be done that there is no risk of fast fracture in the worst condition (lowest temperature including thermal ageing). Also, the effect of the stress-relieving on the pipe behavior will be studied here. To this end, EDF has conducted a research program to demonstrate the fracture resistance of those pipes. The main task of this program consisted of testing three four inches diameter (114.3 mm O.D.) thin butt welded pipes (8.56 mm thick) which are representative of those of the sites.

This paper presents experimental results and the fracture mechanics analyses that were performed for the tests.

TEST DESCRIPTION

Description of the pipes

The base metal of the pipes is the French standard Tu42C carbon-manganese steel. The butt welds were fabricated by manual welding using covered electrodes with a root-pass using the GTAW (Gas Tungsten Arc Welding) process. The materials used were the commercial ESAB OK48.10 for the covered electrodes and NERTAL 60 NUC for the root-pass. The chemical compositions of base and weld metals are listed in table 1.

	C	Si	Mn	P	S	Al	Cu	Mo
Base metal (pipe)	0.18	0.24	0.74	0.014	0.002	0.05	0.04	0.03
Weld metal (welded joint of plate)	0.056	0.28	1.16	0.014	0.003	0.01	0.015	< 0.01
	Ni	**Co**	**Cr**	**V**	**Nb**	**Ti**	**N**	
Base metal (pipe)	0.05	< 0.01	0.13	< 0.01	< 0.01	< 0.01	0.010	
Weld metal (welded joint of plate)	0.02	< 0.01	0.02	0.015	< 0.01	0.01	0.010	

TABLE 1. Chemical compositions of base and weld metal

Those pipes came from remaining stock of a N4 PWR plant and the mockups were manufactured by one of the piping constructors of those plants. So, the welded pipes we tested were representative of the sites. The pipes are four inches diameter (114.3 mm O.D.) and schedule 80 (8.56 mm thick). The specified dimensions of the V weld joint are given in figure 1.

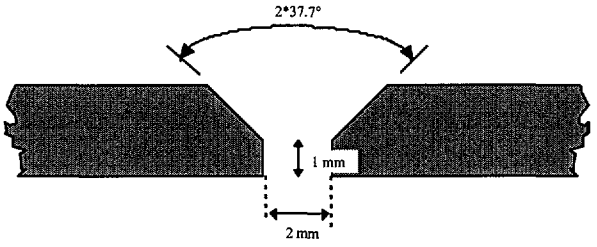

FIGURE 1. Specified dimensions of the V weld joint

The first pipe tested (called ASGMTC1) was in as-welded condition and contained no crack. The second one (called ASGMTC4) was also in as-welded condition and contained a semi-elliptical crack at the outer surface of the middle of the weld joint. This crack was oriented circumferentially in order to be submitted to a tensile stress during the bending test. The third pipe tested (called ASGMTC5) contained the same crack as the second one, but was stress-relieved (1.5 hour at 590°C).

Both cracks were manufactured by electric discharge machining and were not fatigue sharpened in order to be the more identical as possible for an accurate comparison between both cracked pipes. Position and dimensions of the cracks are presented in figure 2. The crack of the third pipe was machined after stress-relieving heat treatment. No geometrical rectification heat was made after the pipes welding.

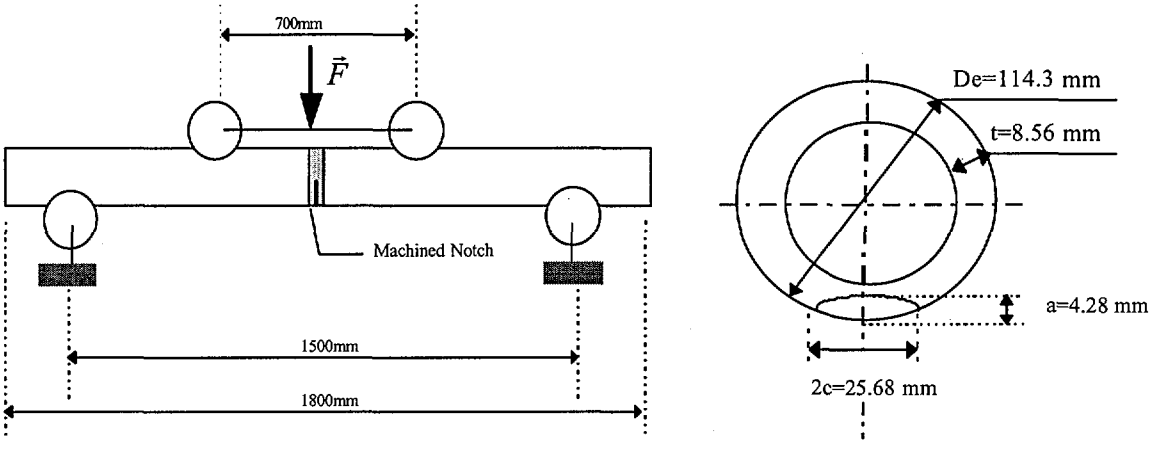

FIGURE 2. Notch location and shape

Description of the test conditions

The three pipes were tested under four point bending conditions (see figure 2) at a temperature of -20°C. With this value of temperature, the most severe in-service conditions are taken into account such as the lowest operating temperature of the pipe (+7°C) and a thermal aged material ($\Delta\theta$ = -25°C which is the conventional and conservative temperature shift taken into account in the plant design report).

The bending load was applied at a quasi-static rate of the ram at 2mm min^{-1} for the uncracked pipe (ASGMTC1) and 1 mm min^{-1} for the cracked pipes (ASGMTC4 and ASGMTC5).

Regarding load, the objective of the tests was to reach the maximum bending moment of the pipes.

Material data

The stress-strain curves of the base metal at room temperature were determined using 6 mm diameter standard tensile specimens. Those specimens were sampled from twin pipe on L direction at as-welded and stress-relieved states. The stress-strain curve of the base metal was also determined at -20°C using 5 mm diameter standard tensile specimen sampled on same direction in the as-welded pipe.

Because of the too small size of the pipe weld joint, 60 mm welded plates were also made, using the same welding material as for the pipes. The stress-strain curves of weld metal at room temperature were determined using 6 mm diameter standard tensile specimens. They were sampled on T direction in the weld joint of the plate.

All stress-strain curves are shown in figure 3, and the conventional tensile properties are given in table 2.

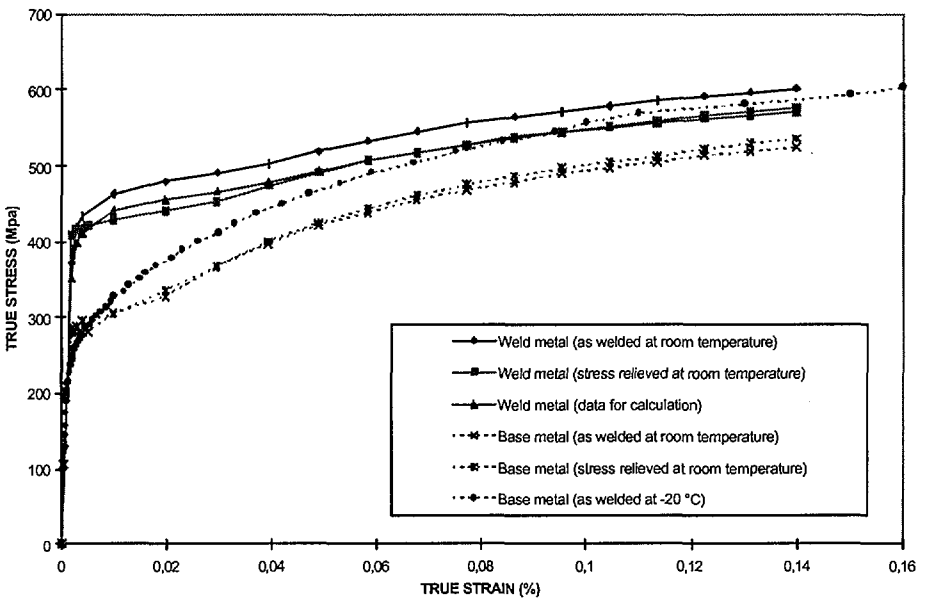

FIGURE 3. True stress - true strain curves for base and weld metal

J-resistance tests for weld metal were made at -20°C as for the test pipes on 0.5T-CT specimens (thickness 12.5 mm with 20% side grooves). A value of $J_{0.2}$ = 405 kJ/m^2 (value of J for 0.2 mm of crack extension) was obtained and the J-R curve was modeled by a linear fit : $J = C1.\Delta a + C2$ where C1 = 911.8 and C2 = 74.

The CT specimens were sampled in the weld joint of the plate (in as-welded condition) with T-S orientation. The tearing resistance tests were carried out according to the GFR procedure (French Fracture Group, 1990) which is the French equivalent to the ASTM

E813 standard.

Material I.D.	Specimen I.D.	Temp. (°C)	0.2% offset yield strength (MPa)	Ultimate tensile strength (MPa)	Young's modulus (GPa)
Weld metal (As-welded plate)	PAS 7	20	433	529	207
	PAS 8	20	426		207
Weld metal (Stress-relieved plate)	PAST 7	20	415	511	206
	PAST 8	20	412	499	206
Base metal (As-welded pipe)	TU2 A	30	279	474	209
	TU2 B	30	279	478	197
Base metal (Stress-relieved pipe)	TU2 AT	20			217
	TU2 BT	20	289	483	208
Base metal (As-welded pipe)	TU1 A	-20	267	511	190
	TU1 B	-20	268	512	212

TABLE 2. Mechanical properties of base and weld metal

Test results

Several measurements were made during the tests. These measurements included applied load, ram displacement, diameter variations (for ovalization), CMOD (at the middle and at the end of the crack), structure rotation (with inclinometers), strains and temperature at different positions of the pipes. The direct current electric potential drop method was used to detect crack initiation. This measurement was made at 9 different positions along the crack region.

The three experiments were conducted till the maximum bending moment of the structure was reached. Applied load versus ram displacement curves we obtained are shown in figure 4 for the three tests. The results are summarized in table 3.

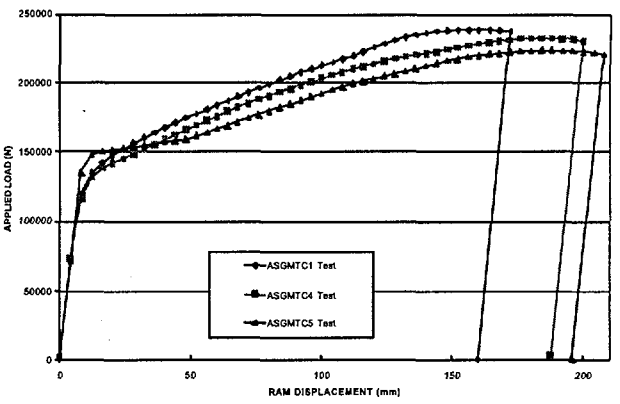

FIGURE 4. Applied load versus ram displacement (test curves)

The maximum bending moment of the first pipe without crack (ASGMTC1) is higher than the second one (ASGMTC4) which is higher than the third one (ASGMTC5). We can explain those differences by the presence of the crack between first and second tests, and by the stress-relieving treatment between second and third ones. However, other differences have to be taken into account. On one hand, some differences between dimensions of the pipes (especially the thickness) which were tested as-cast. Some dimensional readings made at tube ends showed thickness variations that are significant compared to the differences between bending moments. On an other hand, some differences between mockups can also have been introduced by the welding which was a manual one. Those last differences are difficult to evaluate or to quantify.

TEST I.D.	MOCKUP TYPE	MAXIMUM BENDING MOMENT (kN.m)	MAXIMUM APPLIED LOAD (kN)	END OF TEST RAM DISPLACEMENT (mm)	END OF TEST Δa (mm)
ASGMTC1	As-welded No crack	47.6	238	172	---
ASGMTC4	As-welded With crack	46.4	232	200	max < 0.2
ASGMTC5	Stress-relieved With crack	44.6	223	208	max = 0.63

TABLE 3. Main results of the tests

The circumferential machined notches of the two last tests were placed in the zone of maximum axial tensile stress. No evolution of center crack electric potential drop versus ram displacement occurred during the experiments. Post tests examination of the cracks were made. The notch area was cut down from the pipes, then thermally marked, cooled in liquid nitrogen to insure brittle fracture, and finally broken open. These examinations showed that, despite the large amount of loading, the final crack extension reached 0.2 mm for the as-welded pipe and 0.63 mm for the stress-relieved one. Those small values, which correspond to the maximum one along the crack front, were found at the deepest point (see figure 5). That allowed us to conclude that the initiation occurred at the end of the test, so for a loading corresponding to the maximum bending moment.

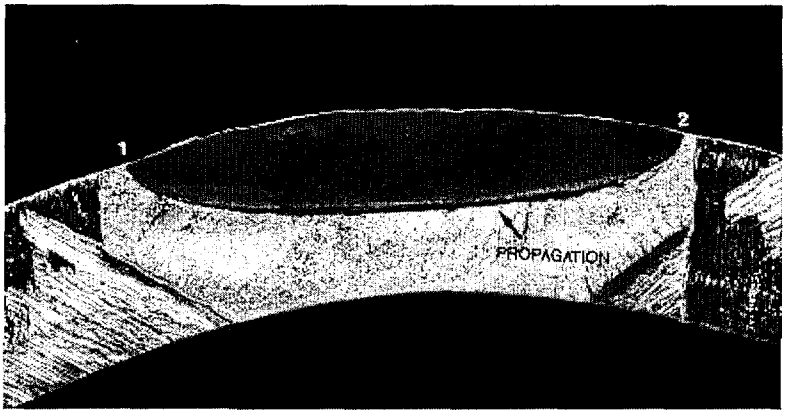

FIGURE 6. Post-test examination of ASGMTC4 crack

Lastly, fractographs showed that both fracture surfaces corresponded to a ductile behavior. Note that, despite the fact the three pipes were severely loaded (we recorded strains up to 5%, see also figure 6) at a low temperature, no brittle fracture occurred.

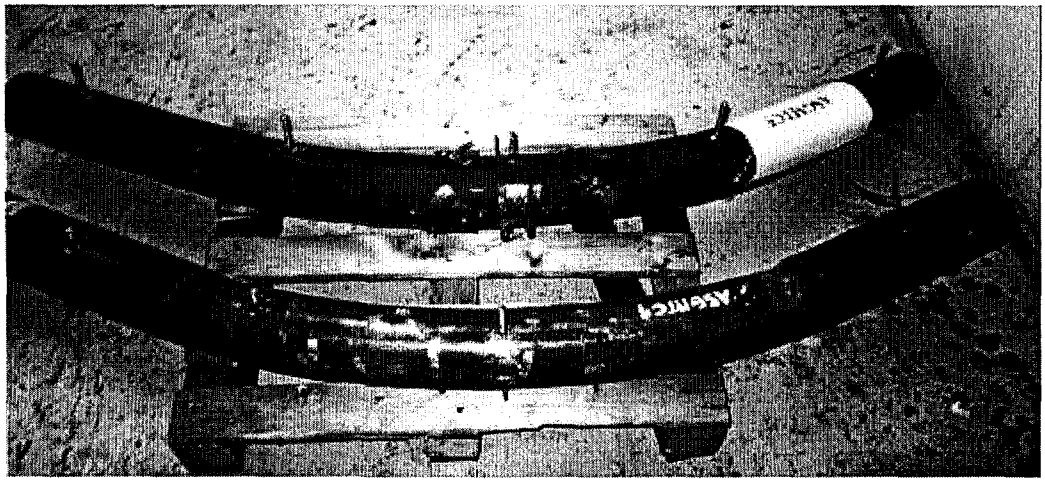

FIGURE 7. ASGMTC4 and ASGMTC5 pipes after tests

NUMERICAL ANALYSIS

Description of the FE models

The aim of the computations was to show their ability to simulate the test and, especially, to predict crack initiation. So, the calculation focused on the tests with cracked pipes (ASGMTC4 and ASGMTC5).

We used the F.E. code named Code_Aster® developed by EDF (Levesque et al., 2000). This general purpose program is mainly devoted to industrial applications. The experiments were modeled using an incremental elastic-plastic 3D finite element calculation. The mesh was built up using solid elements (15 or 20 node elements). A normal integration scheme was used. The mesh was constructed from a cracked block (see figure 7) which was developed for fracture mechanics analyses (global approach).

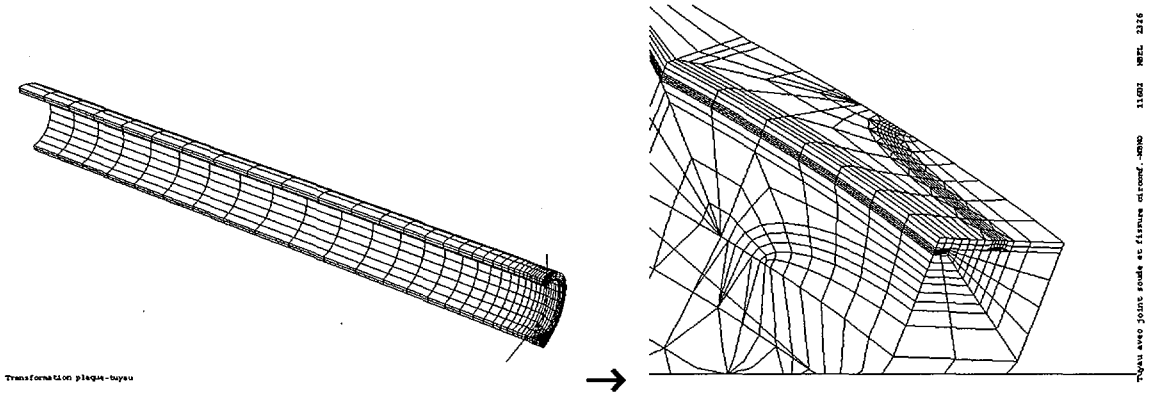

FIGURE 7. Pipe mesh with zoom of the crack region

The model was limited to a quarter structure according to the two symmetries of the mockup. It is particularly refined in the crack area with 16 elements along the half crack front. The section of these elements is a 0.2 x 0.2 mm square. The mesh takes into account the welded joint according to the geometry given in figure 1. There are about 12000 nodes in the model.

For the base metal part of the model, we used the stress-strain curve obtained at -20°C for this material (see figure 3).

For the weld metal part, we only had the stress-strain curve at room temperature. So a preliminary calculation from the CT tests (made at -20°C) was made in order to adjust the stress-strain to use for the calculation.

Global behavior of the tested structure

In this section, we will first focus on the overall behavior of the structure which is assessed in terms of load versus ram displacement curves. In a second time, the crack initiation will be evaluated.

The figure 8 compares the ASGMTC4 and ASGMTC5 tests curves with the calculated curves, first with a small displacement elastic-plastic calculation and, secondly, with a large displacement formulation.

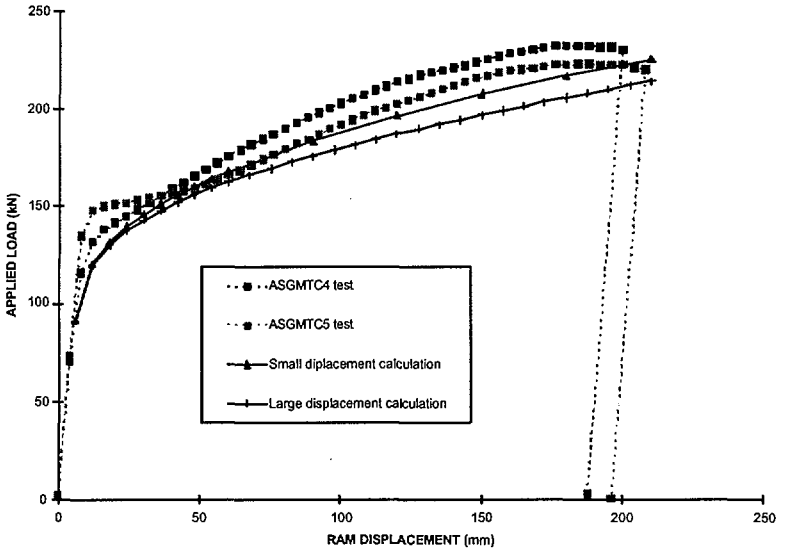

FIGURE 8. Applied load versus ram displacement (test and computation curves)

We assumed that the calculation with as-welded material data is available for the comparison with both (as-welded and stress-relieved) pipes. First, as we can see in figure 3, the stress-strain curves for the base metal are almost identical for as-welded and stress-relieved pipes. And, secondly, the base metal constitutes the most part of the mockups (see figures 1 and 2) and so is preponderant in the behavior of the welded pipes. Moreover, calculation with stress-strain curves of as-welded and stress-relieved weld metal gave quasi identical results.

Figure 8 shows that calculated curves are slightly lower than tests curves and that the large displacement calculation curve is lower than the small displacement one. We can see that the small displacement calculation curve is in correct agreement with ASGMTC5 test curve and a little lower than ASGMTC4 one. Two main reasons can explain this small deviation. The first one, which was recalled before, concerns the mockups geometry. Indeed, the specified dimensions for the mesh are the nominal ones instead of the real pipes dimension (especially thickness) which can significantly vary into fabrication tolerance. This is the main explanation. Moreover, the mesh models an ideal weld joint according to the welding specifications. A second reason can come from material data because we didn't have the exact stress-strain curve for the weld metal as we said before. Also, the model takes into account weld and base metal properties but not HAZ ones.

We used the small displacement calculation to predict crack initiation. For that, we calculated the energy release rate G at the deepest point of the crack versus load. We checked, prior, that the energy release rate G calculated at this point is actually the largest compared to the G values all along the crack front.

The 3D energy release rate was calculated using the G-theta method developed by EDF (Destuynder et al., 1981 ; Wadier and Malak, 1983 ; Suo and Combescure, 1992).

The crack initiation evaluation was made by comparing the material's tearing resistance ($J_{0.2}$ given before) to the energy release rate G at the deepest point of the crack versus load. Then, we compared the initiation crack load given by the pipe tests with the one obtained by calculation (see figure 9). The FE calculation is strongly conservative.

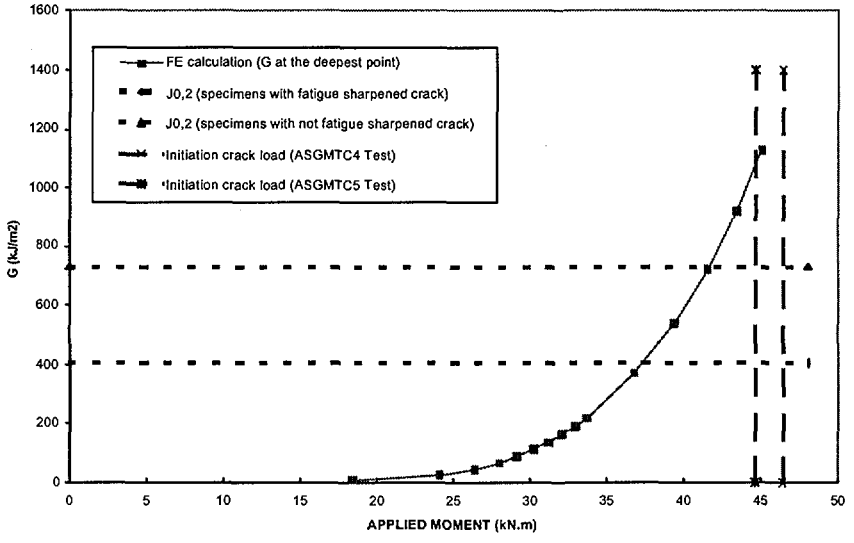

FIGURE 9. Crack initiation prediction with FE energy release rate

In order to give a better coherence to the comparison, another series of J-resistance tests were conducted on 0.5T CT specimens where cracks were manufactured by electric discharge machining (with the same a/w ratio as for the CT specimens mentioned before) but not fatigue sharpened (so as for pipes cracks). We obtained $J_{0.2}$ = 731 kJ/m^2 and a J-R curve fitted by : J = 280.5.Δa + 571.1. With that value, the crack initiation prediction remains conservative but not as strongly as before.

Comparison with RSE-M fracture assessment method

An application of the simplified fracture assessment method of the RSE-M Code (AFCEN, 1997 ; Remond et al., 1997) was made in order to evaluate its performance for this case of cracked pipe.

This method is available to calculate the J-integral in a pipe containing a circumferentially oriented surface crack on the inside or outside surface of a pipe (Le Delliou et al., 2000) submitted to mechanical or/and thermal loads. It derives from R6 rule (Milne et al., 1988).

This method takes into account the material's elastic-plastic behavior by a correction of the plastic area, even for an extensive plasticity as it is the case here. Lr and Kr parameters are calculated using the true stress true strain material curve (same approach as option 2

of the R6 rule). This method is available for a single material, so we choose to take the -20°C base metal stress-strain curve for the present evaluation. Then, the estimation of elastic-plastic J-integral is given by $J = Je/Kr^2$ where Je is the elastic value of J.

We compared the J-integral obtained by this method with the energy release rate G at the deepest point of the crack obtained by finite element as described above. The result is given in figure 11. Both curves are relatively close that shows the simplified method, as well as FE calculation, is conservative in this application.

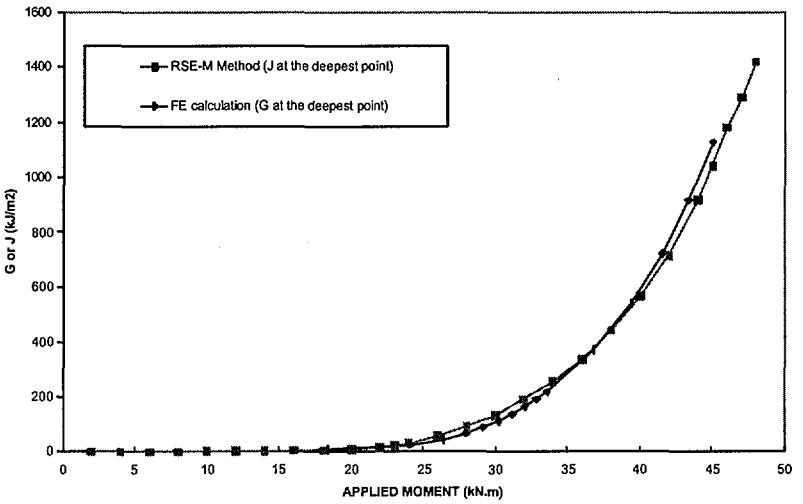

FIGURE 10. Comparison between finite element G and J obtained by RSE-M method

CONCLUSIONS

EDF performed three bending tests on four inches diameter C-Mn steel thin butt welded pipes which are representative of those of French PWR plants. Those pipes were tested at a temperature of -20°C and were loaded till their maximum bending moment was reached. Two of those pipes contained a half thickness semi-elliptical crack in the middle of the weld joint. Despite the large loading at a low temperature, no brittle fracture occurred, the behavior remained ductile and the final crack extensions were very small (0.2 and 0.63 mm maximum at the deepest point). No significant differences appeared between as-welded and stress-relieved pipes.

The finite element analysis was in correct agreement with tests results in terms of global behavior and gave a conservative crack initiation prediction using the energy release rate given by the G-theta method. The J-integral calculated with the simplified fracture assessment method of the RSE-M Code is close to the finite element energy release rate and so, is conservative too.

References

[1] French Fracture Group, 1990
« Test recommendations for measurement of the ductile tearing resistance of metallic materials (J-Δa tests)».

[2] Levesque, J.R., Boin, M., Champain, E., 2000
« Code_Aster® version 5 »
Information brochure in French, EDF report HI-75/2000-009.

[3] Destuynder, Ph., Djaoua, M., 1981
« Sur une interprétation mathématique de l'intégrale de Rice en théorie de la rupture fragile ».
Mathematical methods in applied sciences, 3, pp 70-87.

[4] Wadier, Y. and Malak, O., 1989
« The THETA method applied to the analysis of 3-D elastic- plastic cracked bodies ».
Proceedings SMIRT 10 1989, Anaheim, Vol. G, pp 13-18.

[5] Suo, X.Z., Combescure, A., 1992
« On the application of G(Θ) method and its comparison with De Lorenzi's approach ».
Proceedings Nuclear Engineering and Design, 1992, Vol. 135, pp 207-224.

[6] RSE-M Code, 1997 Edition and 2000 Addenda
« Rules for In-service Inspection of Nuclear Power Plant components ».
AFCEN, Paris.

[7] Remond, A., 1997
« RSE-M, In-service Inspection Rules for the Mechanical Components of PWR Nuclear Islands, Presentation of the 1997 Edition ».
Proceedings ICONE5, paper 2487, Nice, France.

[8] Le Delliou, P, Barthelet, B., Cambefort, P., 2000
« RSE-M Code progress regarding flaw assessment methods and flaw acceptance criteria».
Proceedings ICONE8, paper 8307, Baltimore, USA.

[9] Milne, I. et al., 1988
« Assessment of the Integrity of Structures Containing Defects ».
Int. J. of Press. Vessels and Piping, Vol. 32, pp 127-134.